

Non Linear Optical Properties, Optimized Structure, Global Reactivates and Mulliken Atomic Charge Studies on 5-Chloro-1-Phenyl-1H-Tetrazole Based on Density Functional Theory with Vibrational Assignment

A.Rajeswari^a, M.K. Murali^{a,*}, A.Ramu^b.

^a PG and Research department of physics, JJ. College of Arts & Science (Autonomous), Pudukottai-622422, Tamil Nadu, India. (Affiliated Bharathidasan University, Thiruchirappalli-620024.)

^b Department of Physics, Ganesar College of Arts and Science, Melaisivapuri-622403, Tamil Nadu, India.

Article Info

Volume 83

Page Number: 252 - 268

Publication Issue:

November/December 2020

Abstract

The vibrational spectra of 5-Chloro-1-phenyl-1H-tetrazole (5CIPTZ) have been recorded in the regions 4000–400 cm^{-1} for FT-IR and 3500–100 cm^{-1} for FT-Raman. The molecular structure, geometry optimization, vibrational frequencies were obtained by the density functional theory (DFT) using B3LYP method with 6-31G and 6-311+G basis sets. The complete assignments were performed on the basis of the potential energy distribution (PED) of the vibrational modes, calculated and the scaled values were compared with experimental FT-IR and FT-Raman spectra. The HOMO and LUMO energy gap reveals that the energy gap reflects the chemical activity of the molecule. The dipole moment (μ), polarizability (α), anisotropy polarizability ($\Delta\alpha$) and first hyperpolarizability (β_{tot}) of the molecule have been reported. Information about the size, shape, charge density distribution and site of chemical reactivity of the molecule has been obtained by molecular electrostatic potential (MEP).

Keywords: 5-Chloro-1-phenyl-1H-tetrazole, DFT, FT-IR, FT-Raman, MEP

Article History

Article Received: 25 October 2020

Revised: 22 November 2020

Accepted: 10 December 2020

Publication: 31 December 2020

Introduction

5-Chloro-1-aryl-1H-tetrazoles are widely used in several disparate areas of research and, commercially, in a variety of drug and herbicide manufactures[1]. Biological

activity is encountered due to the special metabolism of disubstituted tetrazoles and also because, in 5-substituted tetrazolyl compounds, the heterocyclic ring is isosteric with a carboxy group and of similar acidity[3]. Some typical uses of

such tetrazoles are in anti-inflammatory drugs[2], herbicides[4], rocket propellants[5] and photography and polymers[6]. Due to this importance, the title molecule 5-Chloro-1-phenyl-1H-tetrazole (5CIPTZ) was investigated by DFT method. Since density functional theory (DFT) has recently emerged as a compromise between the desired level of accuracy and the demand on computational time.

In these studies, the molecular structure, vibrational spectra and HOMO-LUMO energy gap of Pentylentetrazole (PTZ) were investigated by a concerted approach using matrix isolation vibrational spectroscopy and high-level DFT-based theoretical calculations. Regarding their studies, tetrazoles have been found to be extremely interesting and challenging molecules.

Experimental Details:

The fine sample of 5CIPTZ was obtained from Lancaster Chemical Company, UK, with a stated purity of 99% and it was used as such without further purification. The FT-Raman Spectrum of 5CIPTZ was recorded using 1064 nm line of ND: YAG laser for excitation wavelength in the region 3500-100 cm^{-1} on Thermo Electron Corporation model Nexus spectrometer equipped with FT-Raman module accessory. The FT-IR Spectrum of the title compound was recorded in the region 4000-400 cm^{-1} on Perkin Elmer Spectrophotometer in KBr pellet.

3. Computational Details:

The combination of Vibration spectra with quantum chemical calculation is effective for understanding the fundamental mode of vibration of the compound. The structural

characteristic, stability and energy of the compound under investigation are determined by DFT with the three-parameter hybrid functional (B_3) for the exchange part and the Becke Three Lee Yong-Parr (LYP) and 6-31G, 6-311+G basis sets with Gaussian 09 Program Package. The Cartesian representation of the theoretical force constants has been computed at the fully optimized geometry by assuming the molecule belongs to C_1 point group symmetry. The Transformation of force field from Cartesian to internal local symmetry coordinates, the scaling, and the subsequent normal coordinate analysis (NCA) Calculation of potential energy distributions (PED) has been done on a PC with the VEDA program.

Molecular geometry

The optimised geometry of 5CIPTZ with atom numbering is shown in Fig. 3. The more stable 5CITZ molecule has C_1 point group symmetry. The theoretical and experimental C-C bond lengths in the benzene ring of 5CIPTZ are in the range of 1.40 Å. The Alcalá [7] and Derissen [8] reported that the C-C bond length of the isophthalic acid was in the range of 1.391-1.402 Å and well agreed with the theoretical bond length of the title molecule. The C-H bond lengths are calculated as 1.09-1.08 Å, experimentally reported as 0.930 Å. The substitution of halogen reduces the electron density at the ring carbon atom. The C-Cl bond length is calculated as 1.76 Å, which is longest bond length in the molecule. The theoretical bond angles are in harmony with the experimental bond angles. In particular, the C-C-C bond angles of benzene ring in the title molecule is in range of 120.253-121.162 and well agreed with the

experimental range of bond angles 116.2–124.80. the calculated C-N distance in the tetrazole ring is 1.36 Å. where as 1.43 Å for C7-N1 bond. N-N bonds are assigned at 1.40 Å.

Frontier molecular orbital analysis

The study of frontier molecular orbital is important that ionization potential (I), electron affinity (A), electrophilicity index (ω), chemical potential (μ), electronegativity (χ) and hardness (η) to be put into a MO frame work [9]. These global descriptors η , μ and χ are defined as $\eta = (I - A)/2$, $\mu = -(I + A)/2$, $\chi = (I + A)/2$, where I and A denote the ionization potential and electron affinity of the compounds respectively. The ionization energy (I) and electron affinity (A) can be expressed through HOMO and LUMO orbital energies as $I = -E_{\text{HOMO}}$ and $A = -E_{\text{LUMO}}$. Parr et al. [9] have defined a new descriptor to quantify the global electrophilic power of the compound as electrophilicity index ($\omega = \mu^2/2\eta$) which defines a quantitative classification of global electrophilic nature of a compound. The calculated values have tabulated in table. HOMO is localized over the entire molecule and LUMO is localized over the entire compound. the small value of energy gap reveals the title molecule has more reactive.

Molecular Electrostatic Potential (MEP):

Molecular electrostatic potential (MEP) is most helpful descriptor in understanding sites for electrophilic attack and nucleophilic reactions and for the study of biological recognition process [10] and to predict reactive sites of electrophilic and nucleophilic attacks for the title molecule, MEP at the B3LYP optimized geometry

was calculated. Potential value increases in the order red < orange < yellow < green < blue. The negative (red and yellow) regions of MEP were related to electrophilic reactivity and the positive (blue) regions to nucleophilic reactivity. From the MEP of the title compound it is evident that the negative charge covers the N atoms which belongs to tetrazole molecule group and the positive region is over the H group in phenyl ring.

Mulliken Atomic charge

Although atomic charges in a molecule are not experimentally observable quantities, they are fundamental and useful tools to understand and relate properties of molecules to their structures. Even though Various methods are available to assigning charges have been proposed, Mulliken method is widely used due to its convenient. Mulliken atomic charge [11–13] is defined based on orbitals. For each atom, all electronic charge contributions from orbitals centered at that atom are summed up, and electronic overlap clouds between two atoms are divided equally to the two atoms. However, they are extremely basis-function dependent: changing basis functions could result in a big difference for the charge on the same atom [14,15]. In this study two different basis sets were used to find the Mulliken atomic charge of title molecule. They are tabulated in table. All the N atoms got negative charge except N2 atom. As well as all the C atoms got negative charge except C12 atom. Further, all the H atoms got positive charge and Cl atom got negative charge.

Nonlinear optical properties

In the current study, the nonlinear optical (NLO) effect is considered most important because it provides key functions of optical modulation, optical switching, optical logic, and optical memory for the emerging technologies in the areas of telecommunications, optical interconnections, and signal processing [16]. In order to investigate the effects of the HF and DFT/B3LYP methods on the NLO properties of the studied compound, the dipole moments (μ), the polarizabilities (α), the anisotropy of the polarizabilities ($\langle \Delta\alpha \rangle$), and the mean first-order hyperpolarizabilities (β) of 5CITZ were calculated using the finite-field approach and are presented in Table 5.

The dipole moment, the mean polarizability of the title compound are calculated using Gaussian 09 software and are found to be 6.4941, 6.4675 Debye 6-31G, 6-311+G basis set respectively. The magnitude of the first hyperpolarizability from Gaussian 09 output is 0.9636×10^{-30} , 0.9552×10^{-30} esu 6-31G, 6-311+G basis set respectively. The β value calculated by the DFT/B3LYP method shows that the title compound is an attractive molecule for future studies of NLO properties. Based on NLO properties of (common values) urea; the mean first-order hyperpolarizability and polarizability values of the studied molecule are bigger than those of urea.

Vibrational assignment

The detailed vibration assignments of fundamental modes of 5CIPTZ with observed and calculated frequencies and normal modes description are reported in Table 2. The observed experimental FT-IR, FT-Raman spectra are shown in Fig 2 and 3 respectively. The higher value of theoretical

vibrations have been reduced by scaled factor 0.9555 for >1500 cm^{-1} , 0.9826 for <1500 cm^{-1} in 6-31G basis set. as well as 0.9642 for >1500 cm^{-1} , 0.9860 for <1500 cm^{-1} in 6-311+G basis set.

Typically, the C-Cl frequency band is absorbed between 850 and 550 cm^{-1} [17]. For the title compound the bands occurred at 490 cm^{-1} in the IR spectrum are assigned as C-Cl stretching mode. According to the DFT theory, these bands are calculated at 479,440 cm^{-1} (6-31G) and 465,430 (6-311+G) cm^{-1} . The PED value of the CCl stretching modes is 45 and 16%. In this case the deformation modes of C-Cl are assigned at 235 cm^{-1} at Raman spectrum, whereas this bands have been observed at 228,218 cm^{-1} (6-31G), 218,212 cm^{-1} (6-311+G) in theoretically.

The C-H stretching vibrational modes of the title compound are expected in the region 3120-3000 cm^{-1} [18]. This study reveals the CH stretching modes are assigned at 3073 cm^{-1} in the Raman spectrum, 3065 cm^{-1} in the IR spectrum and at 3096, 3091, 3081, 3072, 3062 cm^{-1} (6-31G) and 3166, 3160, 3150, 3140, 3129 cm^{-1} (6-311+G) theoretically. The ring stretching vibrational modes are expected in the region 1615-1260 cm^{-1} [18]. In the present case, the ring modes are occurred at 1691, 1339, 1116 cm^{-1} in the IR spectrum and 1599 cm^{-1} in the Raman spectrum. The theoretical calculation showed that mode at 1578, 1569, 1104 cm^{-1} (6-31G) and 1616, 1606, 1291 cm^{-1} (6-311+G). PED contribution of the phenyl ring stretching modes were assigned at 29%, 44% and 62%. The C-H in-plane deformation of Clptz is expected in the range 1270-1045 cm^{-1} [18]. For the title compound the phenyl C-H in-plane deformation CH(Phenyl) are observed at 1244, 1174 cm^{-1} in the in the

IR spectrum. The DFT calculation gives modes at 1209,1202 cm⁻¹ (6-31G) and 1179,1171cm⁻¹ (6-311+G). The C-H out-of-plane deformations are expected in the range [18] 980-740 cm⁻¹[18]. These CHPh modes are observed at 853 cm⁻¹ in the IR spectrum, corresponding calculated values are 1022,1000,860 cm⁻¹ (6-31G) and 998,980,873 cm⁻¹(6-311+G).

DFT computational method gives mode arising from the N-N stretching at 966,937 cm⁻¹ in 6-31G and 957,923 cm⁻¹ in 6-311+G basis set corresponding to the peak at 975,924 cm⁻¹ in IR spectrum. The C-N vibrations is a very critical task, since the mixing of vibrations is possible in this region. Silverstein et al. [19] attributed C-N stretching absorption in the region 1266–1382 cm⁻¹ for aromatic amines. In benzamide the band observed at 1368 cm⁻¹ is assigned to the CN stretching band [20]. In 1,2,4-triazole the band observed at 1390 and 1327 cm⁻¹ are assigned to CN stretching [21]. The C-N stretching modes are reported in the range 1000–1400 cm⁻¹ [22] and in the present case these bands are assigned at 1418,1382 (6-31G) and 1387,1347 (6-311+G) cm⁻¹ theoretically. 1431,1410 cm⁻¹ in IR and 1433 cm⁻¹ in Raman.

Natural Bond Analysis

The Natural bond orbital [23] analyzes is used to understand the delocalization of electron density and second order donor-acceptor energy. Typically, the stabilization of orbital interaction is high for higher energy differences between interacting orbitals. Effective donor and effective acceptor have this strong stabilization [24-27]. According to the second order perturbation approach, the

stabilization energy is derived [28]. The energy from (donor) i → (acceptor) j is calculated as

$$E^2 = \Delta E_{ij} = q_i \frac{F(i, j)^2}{\varepsilon_j - \varepsilon_i}$$

Where, q_i is the donor orbital occupancy, ε_i , ε_j are diagonal elements (orbital energies) and $F(i, j)$ is the off-diagonal NBO Fock matrix element. The NBO analysis gives valuable information about the intra and inters molecule interaction of the molecule [29].

The current work summarizes second order perturbative calculation donor-acceptor interactions based on NBO. This analysis was carried out by observing all possible interaction between lewis and non-lewis NBOs and calculated their stabilization energy (E_2). Donor NBO (i), acceptor NBO (j) and stabilization energy (E_2) are tabulated in Table 5.7. From this table, it is show that the interaction between the Antibonded N2-N3 (NBO 152) and N4-C5 antibond (NBO 155) gives the strongest stabilization, 79.87 kcal/mol and also, antibond C7-C8 (NBO 158) → C11-C12 antibond (NBO 168), antibond C7-C8 (NBO 158) → C9-C10 antibond (NBO 163), lone pair N1 (NBO 40) → N2-N3 antibond (NBO 152) has the highest stabilization energy are 72.4, 69.1, 20.72kcal/mol Respectively.

CONCLUSION

The present investigation thoroughly analyzed the HOMO-LUMO, and vibration spectra, both infrared and Raman of PTZ

molecules with B3LYP method with standard 6-31G and 6-311+G basis sets. All the vibration bands are observed in the FT-IR and F-Raman spectra of the compound are assigned to various modes of vibration and most of the modes have wave numbers in the expected range. The complete vibration assignments of wave numbers are made on the basis of potential energy distribution (PED). The electrostatic potential surfaces (MEP) together with complete analysis of the vibration spectra, both IR and Raman spectra help to identify the structure and symmetry. The excellent agreement of the calculated and observed vibration spectra reveals the advantages over the other method. Finally, calculated HOMO-LUMO energies show that the charge transfer occurs in the molecule, which are responsible for the bioactive property of the biomedical compound PTZ.

References

- [1]. Wittenberger, S.J. Organic Preparations and Procedures Int., 1994,26, 499.
- [2]. Butler, R.N. Adv. Heterocycl. Chem., 1977,21, 323; Singh, H.; Chawla, A.S.; Kapoor, V.K.; Paul, D. and Malhotra, R.K. "Progress in Medicinal Chemistry", Vol. 17, Eds: Ellis, G.P. and West, G.B., Elsevier, Biomedical PRSS, North-Holland, 1980, p. 15 1
- [3]. Wazir, V.; Singh, G.B.; Gupta, R. and Kachroo P.L. J. Ind. Chem SOC., 1991.68, 305.
- [4]. George, E.F. and Riddell, W.D. U.S. Pat. 3,865,570, Chem. Abstr., 1975.83, 54601; Theodoridis, G.; Hotzman, F.W.; Scherer, L.W.; Smith, B.A.; Tymonko, J.M. and Wyle, M.J. Pestic. Sci., 1990, 30, 259, Chem. Abstr., 1991,114,159059v.
- [5]. Barratt, A.J.; Bates, L.R.; Jenkins, J.M. and White, J.R. U.S. Nut. Tech. Inform Serv., AD Rep., 1971, No. 752370, Chem. Abstr., 1973, 78, 124508; Astashinsky, V.M.; Kostyukevich, E.A.; Ivashkevich, O.A.; Lesnikovich, A.I. and Krasitsky, V.A. Combust. Flame, 1994, 96, 286, Chem. Abstr., 1994,120,248733.
- [6]. Schwartz, N.V. J. Appl. Polym. Sci., 1972,16, 2715; Shelkovnikov, V.V.; Myakishev, K.G.; Kovalev, D. V.; Eroshkin, V.I. and Volkov, V.V. Chem. Abstr., 1990,112,207625j.
- [7]. R. Alcalá, Acta Cryst. 28B (1972) 1671–1677.
- [8]. J.L. Derissen, Acta Cryst. 30B (1974) 2764–2765.
- [9]. Parr, R.G., Szentpaly, L.V., Liu, S., 1999. Electrophilicity index. J. Am. Chem. Soc. 121, 1922-1924.
- [10]. R.Dennington II, T.Keith, J. Millam, Gauss View, Version 4.1.2, Semichem, Inc., Shawnee Mission, KS(2007).
- [11]. R. S. Mulliken, J. Chem. Phys., 1955, 23, 1833–1840.
- [12]. R. S. Mulliken, J. Chem. Phys., 1955, 23, 1841–1846.
- [13]. R. S. Mulliken, J. Chem. Phys., 1955, 23, 2338–2342.
- [14]. C. W. Kern and M. Karplus, Journal of Chemical Physics, 1964, 40, 1374–1389.
- [15]. L. C. Cusachs and P. Politzer, Chemical Physics Letters, 1968, 1, 529– 531.
- [16]. C. Andraud, T. Brotin, C. Garcia, F. Pelle, P. Goldner, B. Bigot, A. Collet, Theoretical and experimental investigations of the nonlinear optical properties of vanillin, polyvanillin, and bisvanillin derivatives, J. Am. Chem. Soc. 116 (1994) 2094-2103.
- [17]. Arivazhagan, M., Jeyavijayan, S., 2011. Vibrational spectroscopic, first order hyperpolarizability and HOMO, LUMO studies of 1,2-dichloro-4-nitrobenzene based on Hartree-Fock and DFT calculations. Spectrochim. Acta. 79, 376-383.

- [18]. Roeges, N.P.G., 1994. A Guide to the Complete Interpretation of IR Spectra of Organic Compounds. Wiley, New York.
- [19]. R.M. Silverstein, G.C. Bassler, T.C. Morrill, Spectrometric Identification of Organic Compounds, fifth ed., John Wiley and Sons Inc., Singapore, 1991.
- [20]. R. Shanmugam, D. Sathyanarayana, Spectrochim. Acta 40 (1984) 764–773.
- [21]. S. Genc, N. Dege, A. Cetin, A. Cansiz, M. Sekerci, M. Dincer, Acta Crystallogr. E60 (2004) o1340–o1342.
- [22]. Kundoo, A.N. Banerjee, P. Saha, K.K. Chattopadhyay, Mater. Lett. 57 (2003) 2193–2197
- [23]. S. Muthu, J. Uma Maheswari, Tom Sundius. Spectrochimica acta part

A.Molecular And Biomolecular spectroscopy 106, (2013)299-309.

- A. E. Reed, F. Weinhold. J. Chem. Phys. 83 (1985) 1736-1740.
- [24]. E. Reed, R. B. Weinstock, F. Weinhold. J. Chem. Phys. 83 (1985) 735-746.
- [25]. E. Reed, F. Weinhold. J. Chem. Phys. 78 (1983) 4066-4073.
- [26]. J. P. Foster, F. Weinhold. J. Am. Chem. Soc. 102 (1980) 7211-7218.
- [27]. P. Singh, S. S. Islam, H. Ahmad, A. Prabakaran. J. Mol. Struct. 1154 (2018) 39-50.
- [28]. K.R. Santhy et al. J. Mol. Struct. (2018). DOI.10. 1016/j. molstruc. 2018. 09. 058.

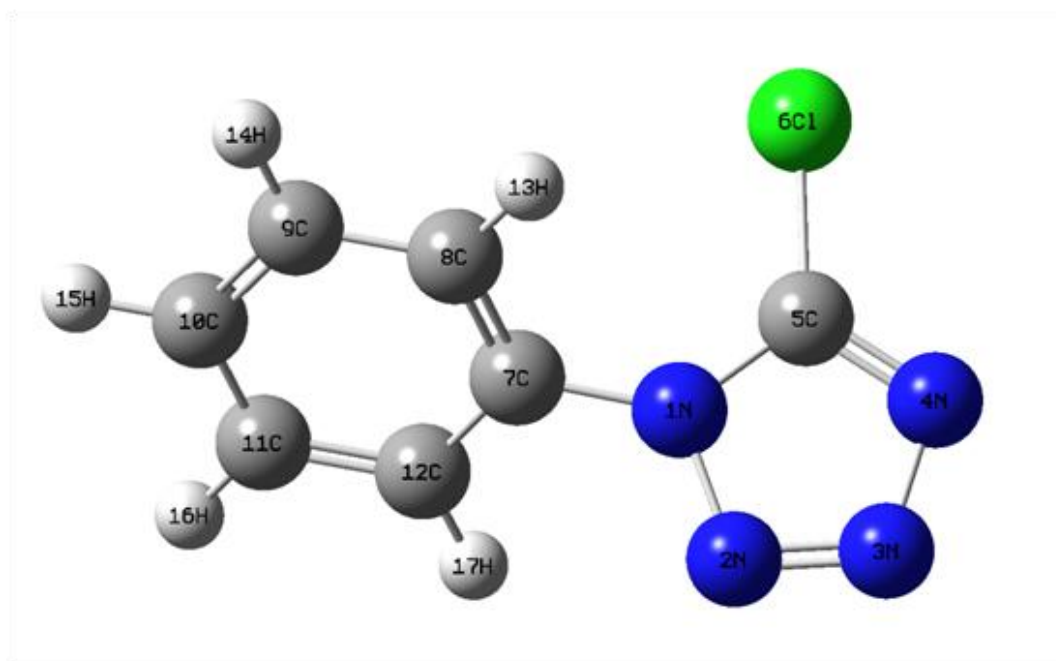


Fig 1. The theoretical geometry structure and atomic numbering scheme of 5-Chloro-1-phenyl-1H-tetrazole (5CIPTZ)

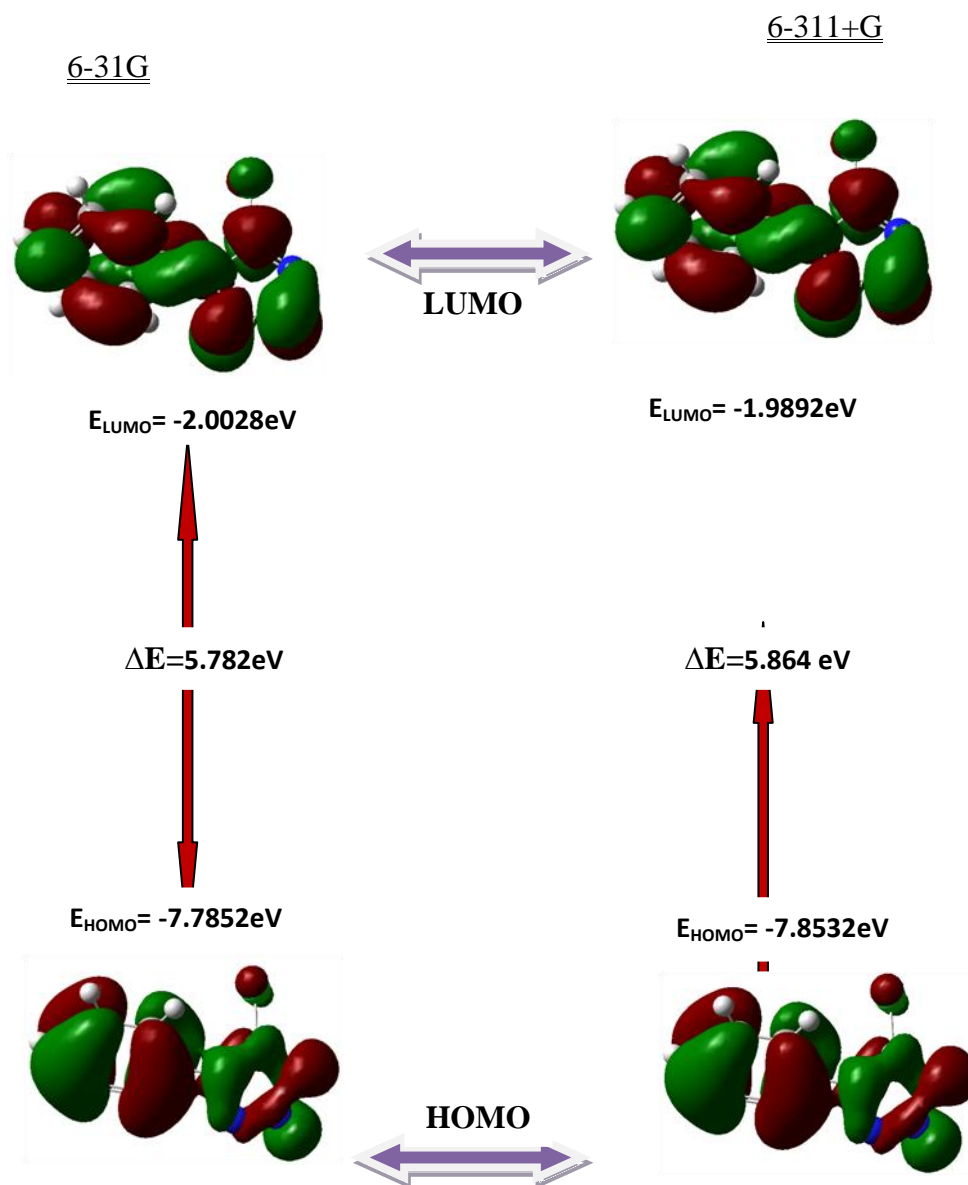


Fig 2: The atomic orbital compositions of the frontier molecular orbital for 5-Chloro-1-phenyl-1H-tetrazole (5CIPTZ)..

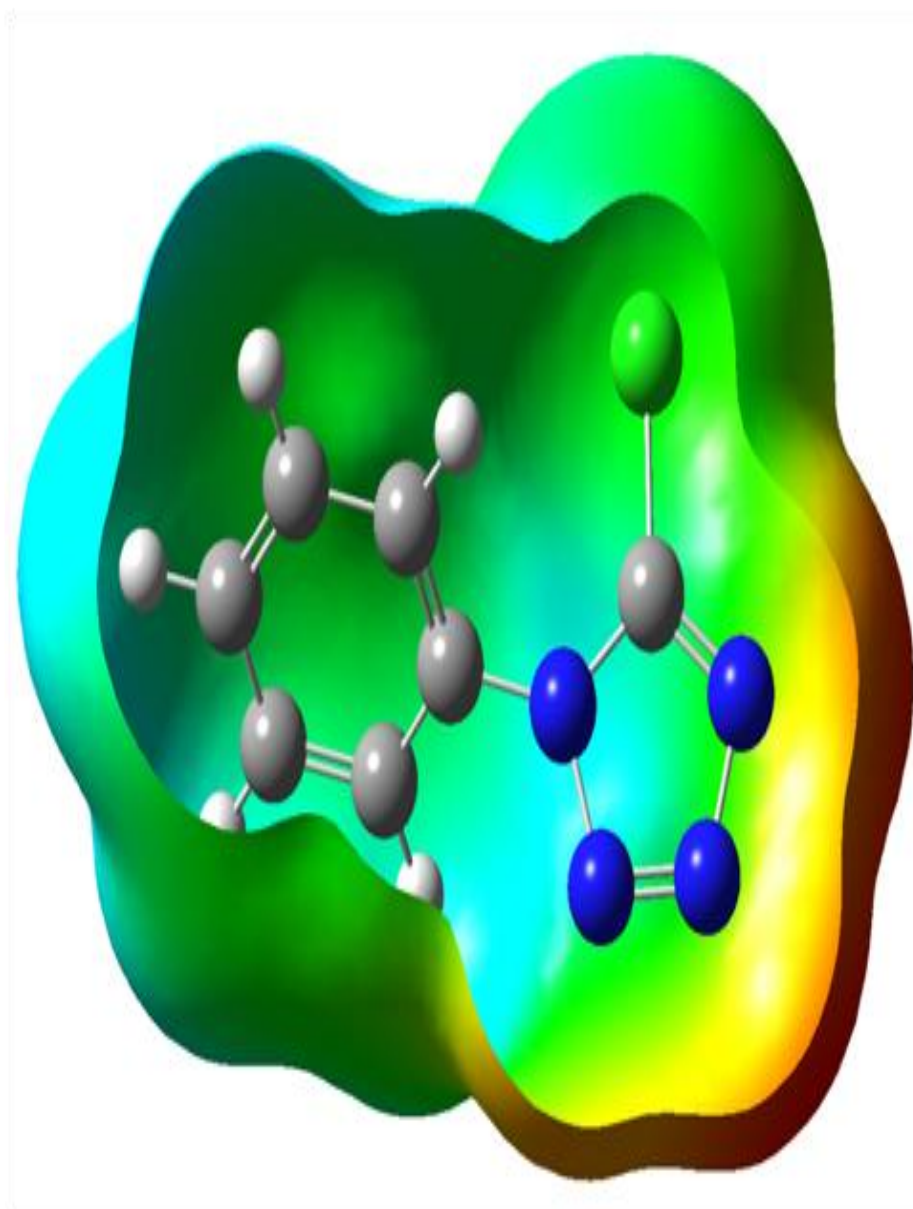


Fig 3. The total electron density surface mapped with of 5-Chloro-1-phenyl-1H-tetrazole (5CIPTZ)

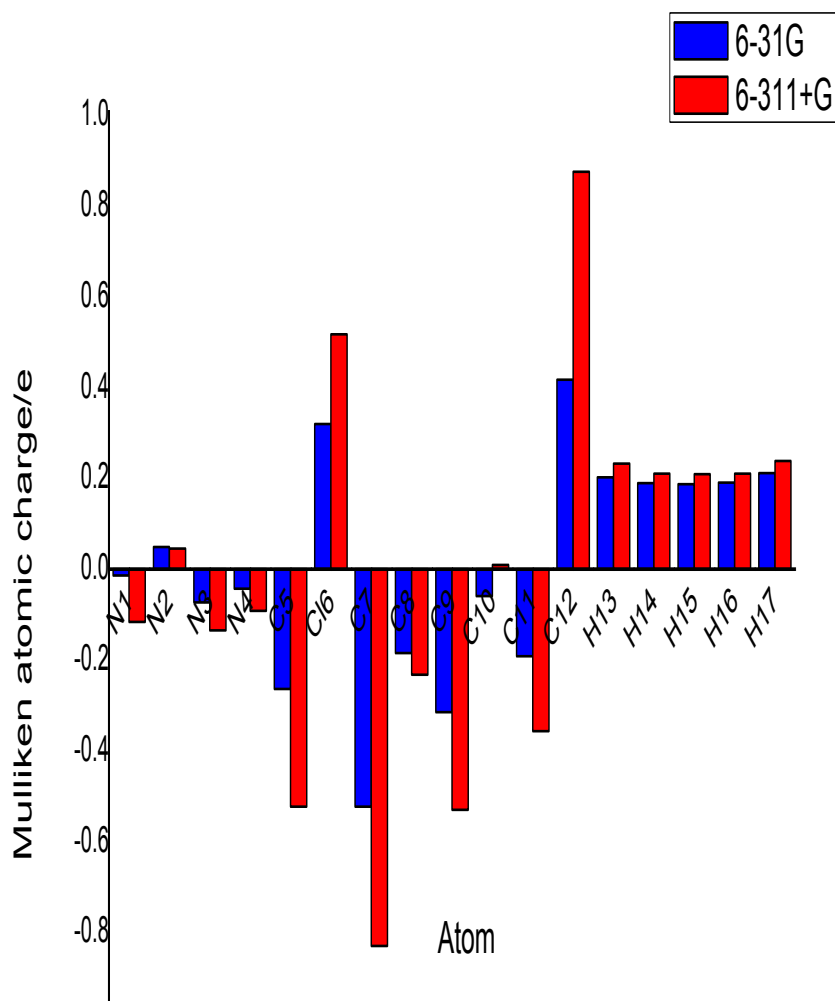


Fig 4 Bar diagram representing the Mulliken atomic charge distribution of 5-Chloro-1-phenyl-1H-tetrazole (5CIPTZ)

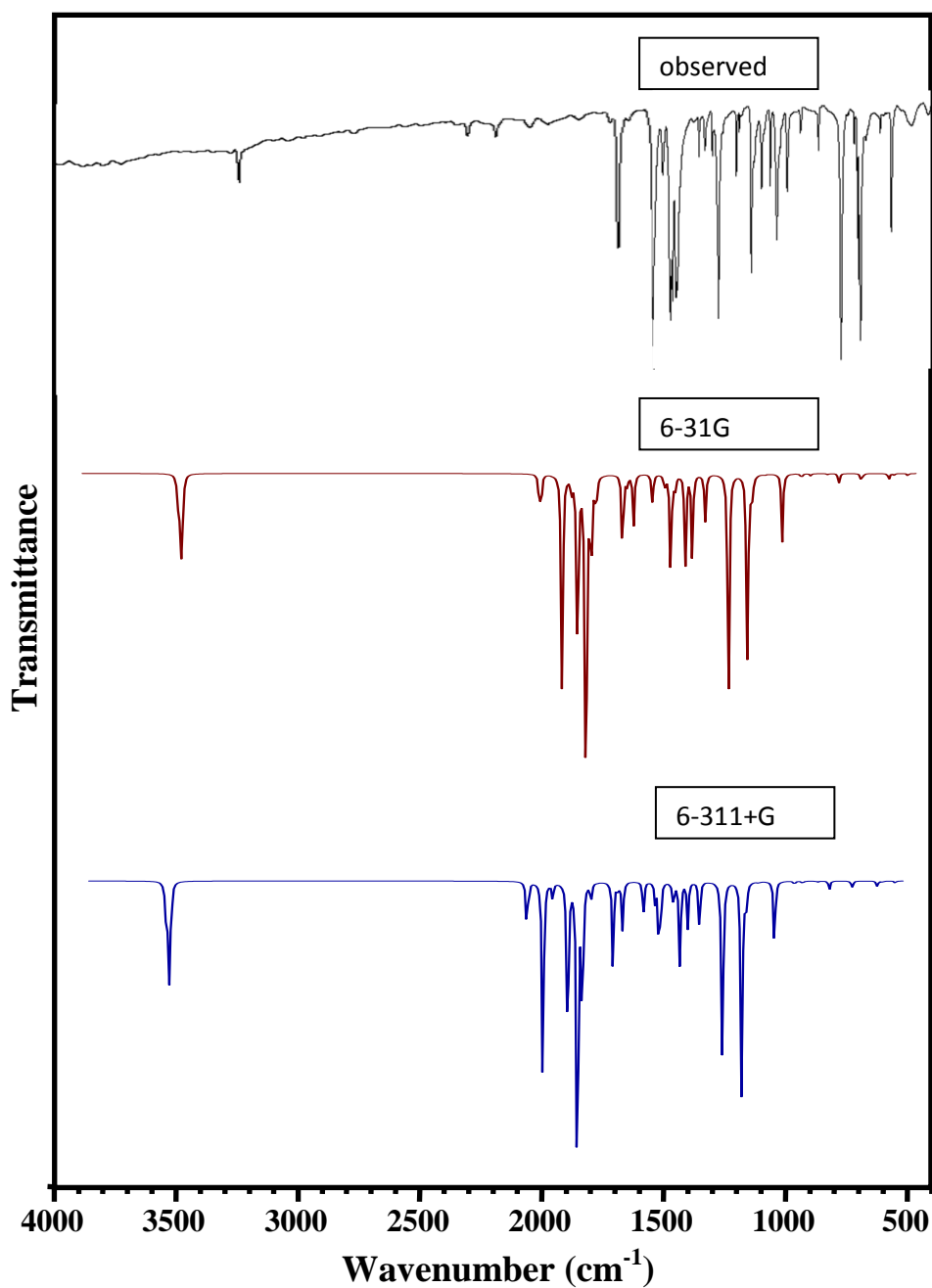


Fig 5. Comparative representation of FT-IR spectra for 5-Chloro-1-phenyl-1H-tetrazole (5CIPTZ).

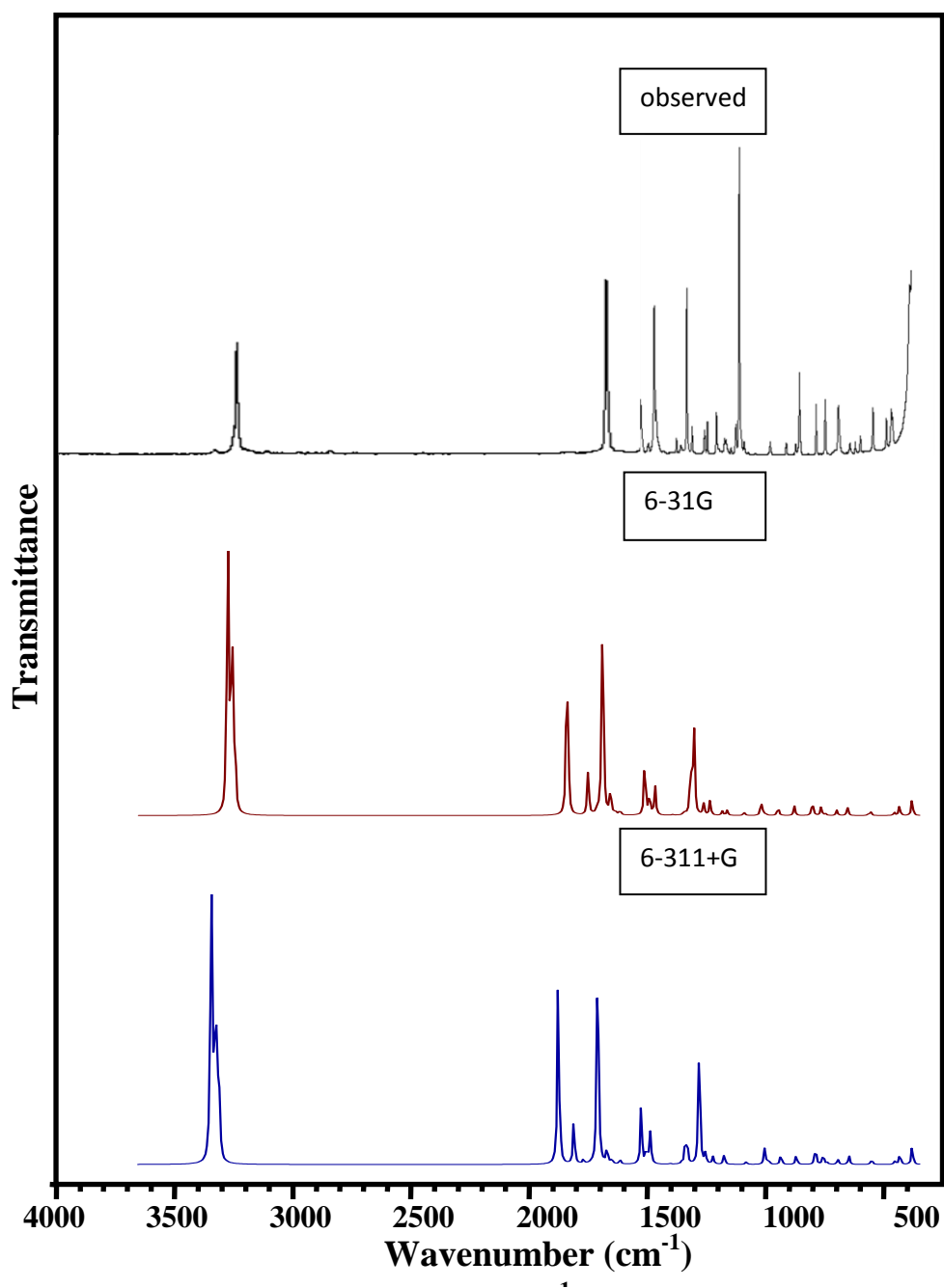


Fig 6. Comparative representation of FT-Raman spectra for 5-Chloro-1-phenyl-1H-tetrazole (5CIPTZ)

Table 1: Geometry Optimization Parameter of 5-Chloro-1-phenyl-1H-tetrazole (5CIPTZ) based on B3LYP/6-31G and B3LYP/6-311+G method and basis set.

BondLength(Å)			BondAngle(°)		
Atom	6-31G	6-311+G	Atom	6-31G	6-311+G
C5-Cl6	1.76	1.76	C5-N1-C7	131.744	131.538
N1-C7	1.43	1.43	N1-C5-Cl6	124.968	124.831
N3-N4	1.40	1.40	N4-C5-Cl6	124.536	124.704
C10-C11	1.40	1.40	N2-N1-C7	121.239	121.269
C9-C10	1.40	1.40	C8-C7-C12	121.214	121.202
N1-N2	1.40	1.40	C11-C12-H17	121.162	121.134
C7-C8	1.40	1.40	C9-C8-H13	120.584	120.593
C7-C12	1.40	1.40	C7-C8-H13	120.296	120.269
C8-C9	1.40	1.40	C8-C9-C10	120.253	120.232
C11-C12	1.40	1.40	C10-C9-H14	120.224	120.213
N1-C5	1.36	1.36	C10-C11-H16	120.217	120.211
N4-C5	1.33	1.32	C10-C11-C12	120.238	120.204
N2-N3	1.32	1.32	C9-C10-C11	120.018	120.039
C10-H15	1.09	1.08	N1-C7-C8	120.087	120.033
C9-H14	1.08	1.08	C11-C10-H15	120.011	120.001
C11-H16	1.08	1.08	C9-C10-H15	119.970	119.959
C8-H13	1.08	1.08	C7-C12-H17	119.687	119.683
C12-H17	1.08	1.08	C12-C11-H16	119.544	119.585
			C8-C9-H14	119.519	119.551
			C7-C12-C11	119.150	119.181
			C7-C8-C9	119.118	119.134
			N1-C7-C12	118.678	118.754
			N2-N3-N4	110.949	110.785
			N1-C5-N4	110.470	110.443
			N2-N1-C5	107.004	107.178
			N1-N2-N3	106.266	106.175
			N3-N4-C5	105.311	105.419

Table 2: HOMO-LUMO energy (eV) and other related properties of 5-Chloro-1-phenyl-1H-tetrazole (5CIPTZ) based on B3LYP/6-31G and B3LYP/6-311+G method and basis set.

Parameters	6-31G (eV)	6-311+G (eV)
Homo(I)	-7.7852	-7.8532
Lumo(A)	-2.0028	-1.9892
Energy gap(ΔE)	5.7824	5.8641
Electronegativity	4.8940	4.9212
Global hardness	2.8912	2.9320
Global softness(eV^{-1})	0.3459	0.3411
Chemical potential	-4.8940	-4.9212
Electriphilicity	4.1420	4.1299

Table 3: Mulliken charge (charge/e) of 5-Chloro-1-phenyl-1H-tetrazole (5CIPTZ) based on B3LYP/6-31G and B3LYP/6-311+G method and basis set.

Atom	6-31G Charge/e	6-311+G
N1	-0.0142	-0.1162
N2	0.0482	0.0448
N3	-0.0734	-0.1347
N4	-0.0431	-0.0923
C5	-0.2643	-0.5233
Cl6	0.3190	0.5174
C7	-0.5227	-0.8294
C8	-0.1844	-0.2327
C9	-0.3151	-0.5296
C10	-0.0595	0.0095
C11	-0.1920	-0.3567
C12	0.4169	0.8746
H13	0.2016	0.2319
H14	0.1899	0.2097
H15	0.1873	0.2090
H16	0.1906	0.2103
H17	0.2117	0.2381

Table 4: Dipole moment(μ), Polarizability(α), Anisotropy polarizability($\Delta\alpha$) and First order polarizability(β_{tot}) of 5-Chloro-1-phenyl-1H-tetrazole (5ClPTZ) based on B3LYP/6-31G and B3LYP/6-311+G method and basis set.

Parameters	6-31G	6-311+G
μ_x	-5.8148	-5.8211
μ_y	2.8346	2.7621
μ_z	-0.5722	-0.5609
α_{XX}	-81.805	-81.9707
α_{YY}	-80.4211	-80.7151
α_{ZZ}	-75.0133	-74.632
α_{XY}	5.8718	5.6262
α_{XZ}	-0.2512	-0.202
α_{YZ}	6.3594	6.4021
β_{XXX}	-85.5234	-85.3691
β_{YYY}	31.8908	31.1578
β_{ZZZ}	-1.4118	-1.2158
β_{XYY}	-13.4878	-12.2542
β_{XXY}	21.7629	21.499
β_{XXZ}	-7.532	-7.3829
β_{XZZ}	4.4195	3.4289
β_{YZZ}	3.2261	3.0377
β_{YYZ}	-7.1489	-7.2038
β_{XYZ}	-7.499	-7.6444
$\mu(\text{debye})$	6.4941	6.4675
$\alpha(\text{esu})$	-11.7038 X10 ⁻²⁴	-11.7077 X10 ⁻²⁴
$\Delta\alpha(\text{esu})$	141.8267 X10 ⁻²⁴	142.1401 X10 ⁻²⁴
$\beta_{tot}(\text{esu})$	0.9636 X10 ⁻³⁰	0.9552 X10 ⁻³⁰

Table 5: Observed Frequency (cm⁻¹), Theoretical Frequency (cm⁻¹) and Vibrational assignment with PED(%) of 5-Chloro-1-phenyl-1H-tetrazole (5CIPTZ) based on B3LYP/6-31G (0.9555, 0.9826) and B3LYP/6-311+G (0.9642, 0.9860) method and basis set.

s.no	Spe cis	Observed Frequency(cm ⁻¹)		Theoretical Frequency(cm ⁻¹)				Vibrational Assignment (PED %)
		FT-IR	FT-Raman	6-31G		6-311+G		
				Calc	scaled	Calc	Scaled	
1	A	-	-	3240	3096	3211	3166	v CH(55)
2	A	-	-	3235	3091	3205	3160	v CH(44)
3	A	-	-	3225	3081	3194	3150	v CH(50)
4	A	-	3073	3215	3072	3185	3140	v CH(72)
5	A	3065	-	3204	3062	3173	3129	v CH(85)
6	A	1691	-	1651	1578	1639	1616	v CC(29)
7	A	-	1599	1642	1569	1629	1606	v CC(44)
8	A	-	-	1552	1483	1545	1524	β HCC(36)
9	A	1502	1503	1511	1444	1503	1482	β HCC(32)
10	A	1431	1433	1443	1418	1439	1387	v NC(35)
11	A	1410	-	1406	1382	1397	1347	v NC(44)
12	A	1404	-	1384	1360	1376	1327	β HCC(22)
13	A	1339	-	1363	1340	1339	1291	v CC(62)
14	A	1267	1269	1251	1229	1245	1200	β NCN(18)
15	A	1244	-	1231	1209	1223	1179	β HCC(37)
16	A	1174	-	1223	1202	1215	1171	β HCC(61)
17	A	1164	1165	1203	1182	1203	1160	v NN(65)+ β CNN(16)
18	A	1116	1119	1123	1104	1114	1074	v CC(21)
19	A	1041	-	1071	1052	1064	1026	β CCC(27)
20	A	1015	-	1046	1028	1047	1010	β NNN(54)
21	A	1003	1004	1042	1024	1039	1002	β CCC(53)
22	A	-	-	1040	1022	1035	998	τ HCCC(50)+ τ CCCC(31)
23	A	-	-	1028	1010	1021	984	v CC(61)
24	A	-	-	1018	1000	1017	980	τ HCCC(37)
25	A	975	-	983	966	992	957	v NN(39)
26	A	924	-	953	937	957	923	v NN(19)
27	A	-	--	898	882	905	873	v NCN(41)
28	A	853	-	876	860	877	873	τ HCCC(55)
29	A	755	-	799	785	803	774	τ HCCC(52)
30	A	-	-	718	705	718	696	τ CCCC(28)
31	A	714	-	717	710	717	694	τ CCCC(38)
32	A	702	-	709	697	701	676	β CCN(47)
33	A	696	699	696	684	696	671	δ NNNC(60)
34	A	612	614	644	633	643	620	τ CCC(46)
35	A	570	568	569	559	571	551	β NCCC(19)
36	A	490	-	487	479	483	465	v CIC(45)
37	A	-	-	448	440	446	430	v CIC(16)

38	A	-	-	427	420	428	413	ν CCCC(69)
39	A	-	-	377	370	379	365	β NCC(13)
40	A	-	327	327	322	327	315	τ CCCC(18)
41	A	-	235	232	228	226	218	β C1CN(21)+ δ CINNC(39)
42	A	-	-	222	218	220	212	β C1CN(20)
43	A	-	-	115	113	114	110	β NCC(24)+ δ NCNC(37)
44	A	-	-	92	90	91	88	β NNC(30)
45	A	-	-	34	33	34	33	δ NNCC(86)

Table 6: Natural Bond Orbital Calculation of 5-Chloro-1-phenyl-1H-tetrazole (5CIPTZ).

S.No	Donor NBO (i)			Acceptor NBO (j)			E(2) kcal/mol	E(j)-E(i) a.u.	F(i,j) a.u.
1	152	BD*	N2-N3	155	BD*	N4-C5	79.87	0.02	0.059
2	158	BD*	C7-C8	168	BD*	C11-C12	72.4	0.01	0.062
3	158	BD*	C7-C8	163	BD*	C9-C10	69.1	0.01	0.063
4	40	LP	N1	152	BD*	N2-N3	20.72	0.33	0.075
5	40	LP	N1	155	BD*	N4-C5	19.44	0.34	0.074
6	8	BD	N4-C5	152	BD*	N2-N3	14.11	0.32	0.062
7	45	LP	Cl6	161	BD*	C8-H13	14.11	0.88	0.1
8	46	LP	Cl6	161	BD*	C8-H13	14.02	0.87	0.1
9	16	BD	C9-C10	158	BD*	C7-C8	11.82	0.28	0.052
10	21	BD	C11-C12	158	BD*	C7-C8	11.69	0.29	0.052
11	46	LP	Cl6	155	BD*	N4-C5	11.25	0.33	0.057
12	16	BD	C9-C10	168	BD*	C11-C12	11.1	0.3	0.051
13	40	LP	N1	158	BD*	C7-C8	10.92	0.41	0.062
14	21	BD	C11-C12	163	BD*	C9-C10	10.83	0.3	0.051
15	42	LP	N3	148	BD*	N1-N2	10.66	0.69	0.076
16	11	BD	C7-C8	168	BD*	C11-C12	10.39	0.32	0.051